Multiple Sclerosis and Related Disorders 36 (2019) 101387

Contents lists available at ScienceDirect

Multiple Sclerosis and Related Disorders

journal homepage: www.elsevier.com/locate/msard

Early neuroaxonal injury is seen in the acute phase of pediatric optic neuritis

Colin Wilbur[a,b], Y. Arun Reginald[c], Giulia Longoni[a,b], Stephanie A. Grover[a], Agnes M. Wong[c], Donald J. Mabbott[d], Douglas L. Arnold[e], Ruth Ann Marrie[f], Amit Bar-Or[e,g], Brenda Banwell[h], Fiona Costello[i], E. Ann Yeh[a,b,j,*], on behalf of The Canadian Pediatric Demyelinating Disease Network.

[a] Division of Neurosciences and Mental Health, SickKids Research Institute, Toronto, Ontario, Canada
[b] Division of Neurology, Department of Pediatrics, The Hospital for Sick Children, Toronto, Ontario, Canada
[c] Department of Ophthalmology and Vision Sciences, The Hospital for Sick Children and University of Toronto, Toronto, Ontario, Canada
[d] Program in Neurosciences and Mental Health, The Hospital for Sick Children and University of Toronto, Toronto, Ontario, Canada
[e] Montreal Neurological Institute, McGill University, Montreal, Quebec, Canada
[f] Departments of Medicine and Community Health Sciences, Max Rady College of Medicine, Rady Faculty of Health Sciences, University of Manitoba, Winnipeg, Manitoba, Canada
[g] Department of Neurology, University of Pennsylvania, Philadelphia, Pennsylvania, United States
[h] Division of Child Neurology, Children's Hospital of Philadelphia and Perelman School of Medicine, University of Pennsylvania, Philadelphia, Pennsylvania, United States
[i] Departments of Clinical Neurosciences and Surgery, University of Calgary, Calgary, Alberta, Canada
[j] Department of Pediatrics (Neurology), University of Toronto, Toronto, Ontario, Canada

ARTICLE INFO

Keywords:
Optical coherence tomography
Multiple sclerosis
Acquired demyelinating syndrome
Optic neuritis

ABSTRACT

Background: Thinning of the retinal nerve fiber layer (RNFL) and ganglion cell/inner plexiform layer (GCIPL) occur in the chronic phase after optic neuritis (ON) in children and reflect neuroaxonal injury. The objective of this study was to describe changes in RNFL and GCIPL thickness in the acute phase following pediatric ON.

Methods: Data were collected prospectively from consecutive children presenting with ON as part of an incident acquired demyelinating event. Children with a final diagnosis of multiple sclerosis (n = 9, 10 ON-affected eyes) or monophasic demyelination (n = 16, 25 ON-affected eyes) who underwent spectral-domain optical coherence tomography (OCT) testing within 30 days of symptom onset were included. Standardized visual assessment was performed at presentation and 6–18 months follow-up. OCT measures were compared to those of healthy controls (n = 25, 50 eyes).

Results: Median (interquartile range [IQR]) global RNFL thickness was increased in ON-affected eyes (155 μm [114–199 μm]) compared to control eyes (104 μm [98.5–107.5 μm]; $p < 0.0001$). Compared to controls, fellow eyes demonstrated a reduced temporal quadrant RNFL thickness (59 μm [53–72 μm] versus 71.5 μm [65–81 μm]; $p = 0.013$) and lower GCIPL thickness (80.5 μm [74–88 μm] versus 87 μm [85–89 μm]; $p = 0.003$). The ON-affected eyes of children with monophasic demyelination demonstrated a greater global RNFL thickness (183.5 μm [146.5–206 μm]) compared to the ON-affected eyes of children with multiple sclerosis (108.5 μm [95–124 μm]; $p = 0.01$). OCT measures at presentation did not predict low-contrast visual acuity nor color vision at 6–18 months follow-up.

Conclusion: Children with multiple sclerosis show less RNFL swelling in their ON-affected eyes at onset compared to children with monophasic demyelination. Lower GCIPL and temporal RNFL thickness in the clinically unaffected eyes of those children with unilateral ON suggests the presence of pre-existing neuroaxonal injury in children presenting with a first episode of ON. This finding may be driven by the subset of children with multiple sclerosis.

Abbreviations: CI, confidence interval; CNS, central nervous system; GCIPL, ganglion cell/inner plexiform layer; HCVA, high-contrast visual acuity; HRR, Hard-Rand-Rittler; IQR, interquartile range; LCVA, low-contrast visual acuity; MOG, myelin oligodendrocyte glycoprotein; MS, multiple sclerosis; NMOSD, neuromyelitis optica spectrum disorder; OCT, optical coherence tomography; ON, optic neuritis; OR, odds ratio; RNFL, retinal nerve fiber layer; SD, standard deviation

* Corresponding author.
E-mail address: ann.yeh@sickkids.ca (E.A. Yeh).

https://doi.org/10.1016/j.msard.2019.101387
Received 27 June 2019; Received in revised form 3 September 2019; Accepted 6 September 2019

1. Introduction

Optic neuritis (ON) occurs at onset in approximately one-quarter of pediatric acquired demyelinating syndromes of the central nervous system (CNS) (Banwell et al., 2009). ON may occur as part of a monophasic inflammatory process or as a manifestation of relapsing disorders such as multiple sclerosis (MS) or neuromyelitis optica spectrum disorder (NMOSD) (Wilejto et al., 2006; Lechner et al., 2016). Approximately half of children presenting with ON have bilateral eye involvement clinically (Wilejto et al., 2006; Absoud et al., 2011). Subclinical optic nerve involvement has been described as a common finding in adult MS (Petzold et al., 2017) and is also frequently observed among children with MS (Pohl et al., 2006).

Optical coherence tomography (OCT) is a non-invasive imaging technique that allows reliable, high-resolution (within 3–5 μm) measurements of retinal structure (Fig. 1). OCT values provide indirect measures of axonal (retinal nerve fiber layer [RNFL] thinning) and neuronal (macular ganglion cell/inner plexiform layer [GCIPL] thinning) injury (Costello and Burton, 2018) and correlate with visual function including high- and low-contrast visual acuity, color vision, and visual fields (Yeh et al., 2014; Sanchez-Dalmau et al., 2018; Costello et al., 2006).

Acute inflammatory lesions of the afferent visual pathway cause retrograde neuroaxonal degeneration, which manifests as distinct patterns of RNFL and GCIPL thinning over time (Kupersmith et al., 2011, 2016). Adult studies have demonstrated that the majority of GCIPL thinning following acute ON occurs by 3 months after onset, while initial RNFL swelling in acute ON proceeds to thinning that is largely maximal after 6 months (Kupersmith et al., 2016; Costello et al., 2015). Additionally, subclinical RNFL and GCIPL thinning can be observed in MS eyes without a history of clinical ON and this can be progressive over time (Gelfand et al., 2012; Graves et al., 2017). The presence of subclinical RNFL and/or GCIPL thinning at the time of a first attack suggests that neuroaxonal injury in the anterior visual pathway occurs during the pre-clinical phase of the disease (Gelfand et al., 2012; Knier et al., 2016). OCT measures in MS can thus be interpreted to represent neuroaxonal injury that is either relapse-related or, alternatively, a manifestation of subclinical disease (Meltzer et al., 2018).

While there is an abundance of evidence supporting the role of OCT as a surrogate marker of neuroaxonal injury in adults, fewer studies of this ocular imaging technique have been performed in children with CNS demyelinating disorders. In this study, we evaluate changes in retinal structure by OCT during the acute phase of ON among children presenting with their first demyelinating event, and whether these findings differ in children diagnosed with MS compared to those with monophasic demyelination. We also aimed to investigate the relationship between these early OCT measures and functional visual outcomes in this pediatric cohort.

2. Materials and methods

2.1. Study population and design

Study participants included consecutive children presenting with acute ON from 2010 to 2017 captured prospectively through a patient registry in the Neuroinflammatory Disorders Clinic at The Hospital for Sick Children (Toronto, Canada). Children were included if they met all of the following criteria: (1) ON as part of an incident acquired demyelinating syndrome; (2) diagnosis at last follow-up of MS or monophasic demyelination; (3) age less than 18 years at the time of ON diagnosis; (4) OCT assessment performed within 30 days of reported ON symptom onset. Children were excluded if they had any of the following: (1) neurologic dysfunction secondary to a cause other than acquired CNS demyelination (e.g. CNS infection, primary CNS vasculitis); (2) diagnosis at last follow-up of NMOSD or other recurrent CNS demyelination not fulfilling MS criteria; (3) any ocular abnormality that may influence the interpretation of OCT results, such as congenital or acquired retinal abnormalities, refractive error greater than 6.00 diopters, a history of ocular trauma, or alternative causes of vision loss (including congenital color vision deficiencies).

Healthy control children (aged 8–18 years) were recruited from 2011 to 2018 and included if they had no history of significant neurocognitive disability, neurologic disease, inflammatory/autoimmune disease, or significant ocular abnormality (as defined above).

2.2. Ethics approval

This study was approved by the SickKids Research Ethics Board and informed consent/assent was obtained from patients and their families.

2.3. Diagnosis of acquired demyelinating syndromes

ON was defined by acute or subacute visual loss (high contrast, low contrast, and/or color vision deficits), associated with pain precipitated by eye movement, a relative afferent pupillary defect, abnormal visual field function in the affected eye(s), and/or optic nerve swelling

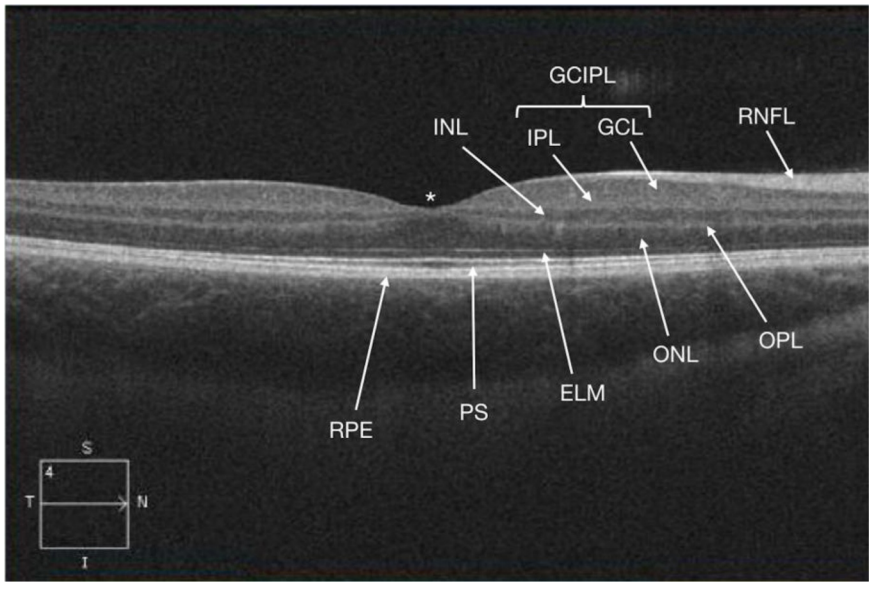

Fig. 1. Macular optical coherence tomography scan (Cirrus HD-OCT), centered through the fovea (*). From outer-to-inner, the retinal layers visualized are: retinal pigment epithelium (RPE); photoreceptor layer (PS); external limiting membrane (ELM); outer nuclear layer (ONL), outer plexiform layer (OPL), inner nuclear layer (INL); inner plexiform layer (IPL); ganglion cell layer (GCL); retinal nerve fiber layer (RNFL). The combined measure of the GCL and IPL is reported as the ganglion cell/inner plexiform layer (GCIPL).

detected on fundus examination. Diagnosis at most recent evaluation was classified using established diagnostic criteria as: MS, NMOSD, other recurrent CNS demyelination, or monophasic demyelination (defined as those not fulfilling MS or NMOSD criteria and having no recurrence of demyelination more than 30 days after onset of the initial event) (Krupp et al., 2013; Wingerchuk et al., 2015). Clinical testing was performed through commercial laboratories using cell-based assays for aquaporin-4 antibody (Medimmune, The Hospital for Sick Children) and myelin oligodendrocyte glycoprotein (MOG) antibody (Immunology Laboratory, Oxford) (Waters et al., 2014; Waters et al., 2015). Those children who were seropositive for anti-MOG antibodies were classified as having non-MS diagnoses.

2.4. Clinical data

Clinical data were collected using standardized case report forms and included: sex, date of clinical onset, age at clinical onset, presumed diagnosis at presentation, diagnosis of unilateral or bilateral ON, occurrence of subsequent demyelinating relapses, and final diagnosis at last follow-up.

2.5. Optical coherence tomography (OCT) testing

OCT scan performed within 30 days of symptom onset was analyzed for all included ON participants. If a participant had multiple OCT scans, only the first was analyzed. OCT scans were obtained for ON participants and control subjects and were performed by a single trained technician using the spectral domain OCT Cirrus scanner (Model 4000, software v7.0.3.19, Carl Zeiss Meditec) in a dark room with dilated pupils. Scans with a minimum signal strength of 7 (out of 10) were included and considered acceptable if correctly centered with appropriate illumination and no overt artifact (Tewarie et al., 2012; Schippling et al., 2015). Serial optic disk (200 × 200) and macular cube (512 × 128) protocol scans quantifying a 6 × 6 × 2-mm volume were obtained for each eye, without eye tracking. Global and quadrant peripapillary RNFL thicknesses were measured from a 1.7 mm-radius circle centered on the optic nerve head and reported in micrometers. The average, minimum, and sectoral (superotemporal, superior, superonasal, inferonasal, inferior, and inferotemporal) GCIPL thicknesses were measured in an elliptical annulus around the fovea (vertical inner and outer radius 0.5 mm and 2 mm, respectively; horizontal inner and outer radius 0.6 and 2.4 mm, respectively) (Mwanza et al., 2011). Mean macular GCIPL thickness was calculated using the OCT machine manufacturer's included automated segmentation software and reported as GCIPL thickness in micrometers. Manual correction of segmentation was not performed.

2.6. Functional visual assessment

Patient and control eyes were tested monocularly and sequentially; screening for refractive error was performed for each eye. High-contrast visual acuity (HCVA), low-contrast visual acuity (LCVA), and color vision were assessed at presentation and at follow-up 6–18 months (mean 381 ± 100 days) following ON onset. If visual testing was documented at multiple time points during this follow-up period, the assessment closest to 12 months after initial presentation was analyzed. Participants experiencing ON recurrence prior to this follow-up examination were excluded from this analysis of long-term visual outcomes. HCVA was assessed using the modified Pediatric Eye Disease Investigator Group Amblyopia Treatment Study protocol (Holmes et al., 2001), Early Treatment Diabetic Retinopathy Study charts (Ferris et al., 1982), or wall-mounted Snellen chart at 20 feet. LCVA was assessed with a wall-mounted Pelli-Robson chart or the M&S Smart System II (MSSS-II; M&S Technologies Inc, Niles, IL), which have been demonstrated to have good agreement (Chandrakumar et al., 2013), and reported as log units. For the Pelli-Robson chart, final LCVA was recorded as the lowest contrast sensitivity for which the participant correctly identified at least 2 of 3 letters at the same contrast level. For the MSSS-II, final LCVA was recorded as the lowest percent contrast at which the participant could correctly identify 2 of 3 randomly selected Sloan letters. Color vision was assessed using Hardy-Rand-Rittler (HRR) plates and the number of objects correctly identified in the first 6 screening plates was scored for patients and control subjects.

2.7. Statistical analysis

Eyes were classified as ON-affected eyes, fellow eyes (clinically unaffected eyes in those participants with unilateral ON), and healthy control eyes. Continuous variables were summarized as mean (standard deviation [SD]) or median (interquartile range [IQR]) as appropriate, and categorical variables as frequency (percentage). Demographic characteristics of cases and controls were compared using student's t tests, Chi-squared tests, or Fisher's exact tests as appropriate. Correlations between global RNFL and GCIPL thickness were assessed using Spearman's rank correlation coefficient (ρ) for affected and fellow eyes, separately.

RNFL (global and quadrant) and GCIPL thickness in ON-affected and fellow eyes at presentation were compared to healthy control eyes. Generalized linear mixed models were fitted using an unstructured covariance matrix to account for potential within-subject correlations. Multivariable linear mixed models were fitted to compare individual OCT measures (dependent variables: global RNFL thickness, quadrant RNFL thickness, and GCIPL thickness) by eye type (ON-affected or fellow eyes versus control eyes), while accounting for sex and age (years). RNFL models were log-transformed, to account for skewed distribution of values in the patient group. The relationships between the time from ON onset to OCT testing and global RNFL thickness and GCIPL thickness in ON-affected eyes were also assessed using generalized linear mixed models, accounting for potential within-subject correlations. Next, OCT measures at presentation were compared between children diagnosed with MS to those with monophasic demyelination. Multivariable linear mixed models were fitted to compare OCT measures (dependent variables: global RNFL, temporal quadrant RNFL, and GCIPL thickness) by diagnostic group (MS or monophasic demyelination) in ON-affected and fellow eyes, adjusting for sex and age (years). These models were also used to compare OCT measures in those children diagnosed with MS to those with anti-MOG seropositive monophasic demyelination.

As a secondary outcome, LCVA (continuous variable) and color vision (analyzed categorically as normal if all color plates correct or abnormal if one or more plates was incorrect) assessed at 6–18 months follow-up were compared between ON-participant and control eyes using Kruskal-Wallis test for continuous variables and Fisher's exact test for categorical variables. Generalized linear mixed models were then fitted to assess the relationship between LCVA or color vision at follow-up (dependent variables) and global RNFL or GCIPL thickness at presentation in ON-participants, adjusted for age at follow-up (years), sex, and eye type at presentation (ON-affected or fellow).

Statistical analysis was performed using SAS v9.4 (SAS Institute Inc., Cary, NC, USA). Boxplots were created using R version 3.3.2 (R Core Team, 2016) with the Beeswarm package. Post-hoc adjustment for multiple comparisons was performed according to the Benjamini-Hochberg procedure, with a false discovery rate of < 0.05 (Benjamini and Hochberg, 1995).

3. Results

3.1. Study population

Twenty-five ON-participants (35 ON-affected and 15 fellow eyes) were included and compared to 25 healthy controls (50 eyes, Fig. 2, Table 1). Sixteen children with monophasic demyelination were

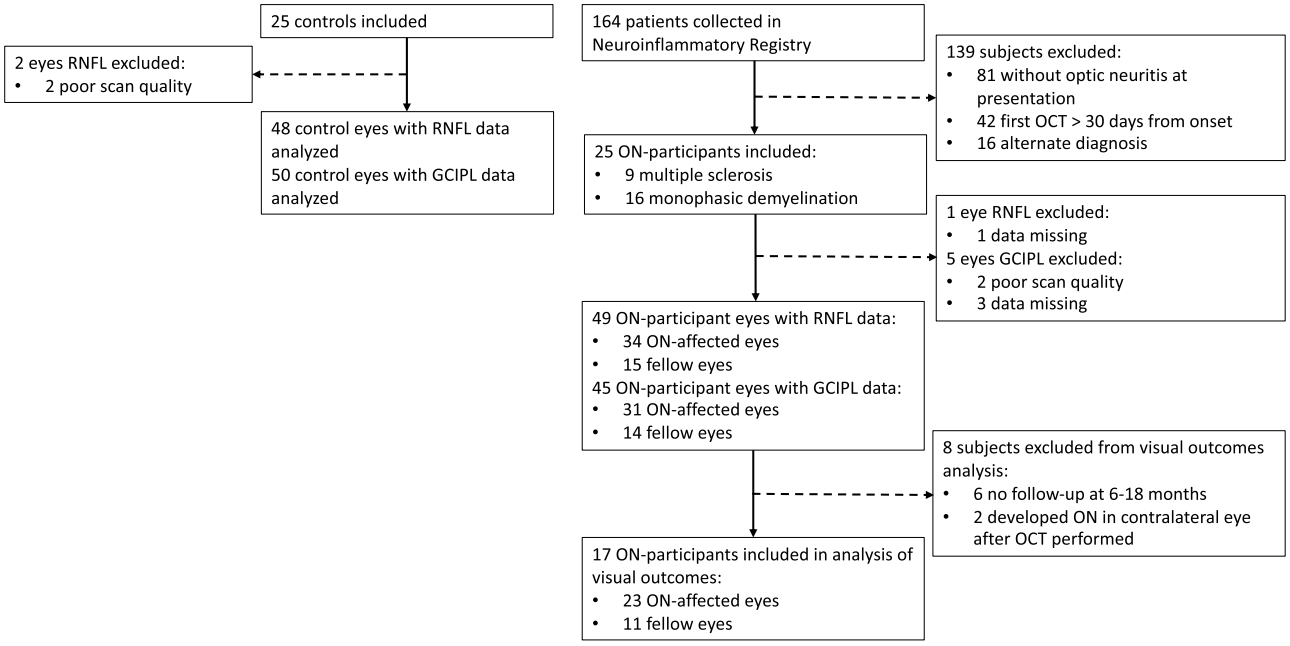

Fig. 2. Study flowsheet. GCIPL = ganglion cell/inner plexiform layer; ON, optic neuritis; RNFL, retinal nerve fiber layer.

included, having no recurrent demyelinating attacks after median follow-up of 16 months (IQR 9–24 months). Ten children were seropositive for anti-MOG antibody, of whom six presented with bilateral ON. Results of follow-up anti-MOG antibody testing performed outside of the acute phase were not available. At presentation, 12 ON-participants (48%) had a HCVA worse than 20/200 in at least one affected eye. Twenty-two participants received pulse intravenous methylprednisolone a median 8 days (range 0–31 days) following ON onset.

3.2. Peripapillary RNFL thickness

OCT testing was performed a median 10 days (range 0–29 days) from symptom onset. Fifteen participants had received intravenous methylprednisolone prior to OCT testing, with the first dose administered a median 2 days (range 0–11 days) prior to OCT. There was no significant association between the time from ON onset to OCT testing and global RNFL thickness in ON-affected eyes ($\beta = -0.02$, $p = 0.06$). Lower global RNFL thickness correlated moderately with lower GCIPL thickness in ON-affected eyes ($\rho = 0.57$; 95% CI 0.16, 0.81; $p = 0.001$), while a very strong correlation was demonstrated between lower global RNFL thickness and lower GCIPL thickness in fellow eyes ($\rho = 0.85$; 95% CI 0.54, 0.97; $p = 0.0001$).

Global RNFL thickness was greater in ON-affected eyes (median 155μm [IQR 114–199μm]) compared to control eyes (median 104 μm [IQR 98.5–107.5 μm]; $p < 0.0001$; Fig. 3A). Higher RNFL measures in ON-affected eyes compared to controls were also seen in the superior, inferior, and nasal quadrants (Table 2). In comparison to control eyes, fellow eyes of ON-participants demonstrated a lower inferior RNFL thickness (median 122 μm [IQR 111–140 μm] versus 139 μm [IQR 125–148 μm]; $p = 0.013$) and lower temporal RNFL thickness (median 59 μm [IQR 53–72 μm] versus 71.5 μm [IQR 65–81 μm]; $p = 0.008$; Fig. 3B).

3.3. GCIPL thickness

There was no significant association between the time from ON onset to OCT testing and GCIPL thickness in ON-affected eyes ($\beta = -0.28$, $p = 0.29$). GCIPL thickness was lower in both ON-affected eyes (median 79 μm [IQR 74–88 μm]; $p = 0.003$) and fellow eyes (median 80.5 μm [IQR 74–88 μm]; $p = 0.003$) compared to control eyes (median 87 μm [IQR 85–89 μm]; Table 2, Fig. 4).

3.4. OCT patterns of neuroaxonal injury: comparing diagnostic sub-groups

Global RNFL thickness was lower in the ON-affected eyes of children with MS (median 108.5μm [IQR 95–124 μm]) compared to the ON-affected eyes of children with monophasic demyelination (median 183.5 μm [IQR 146.5–206 μm]; $p = 0.01$). Remaining OCT measures in ON-affected and fellow eyes did not differ significantly between those children with MS compared to those with monophasic demyelination (Table 3). When the ON-affected eyes of children with MS were compared to only those ON-affected eyes of children seropositive for anti-MOG antibody, global RNFL thickness remained lower in the MS group, but this difference was not statistically significant after correction for multiple comparisons (median 108.5μm [IQR 95–124 μm] versus median 158 μm [IQR 135–199 μm]; $p = 0.04$).

Table 1
Participant demographics and clinical characteristics.

	ON-Participants ($N = 25$)	Controls ($N = 25$)
Female, n (%)	17 (68)	17 (68)
Age (years), mean (SD)	12.4 (3.5)	13.8 (2.6)
Diagnosis, n (%)		–
Multiple Sclerosis	9 (36)	
Monophasic Demyelination	16 (64)	
Myelin Oligodendrocyte Glycoprotein Antibody, Number positive / Number tested (%)	10/19 (53)	–
Aquaporin-4 Antibody, Number positive / Number tested (%)	0/17 (0)	–
Simultaneous Bilateral ON, n (%)	10 (40)	–

ON, optic neuritis.

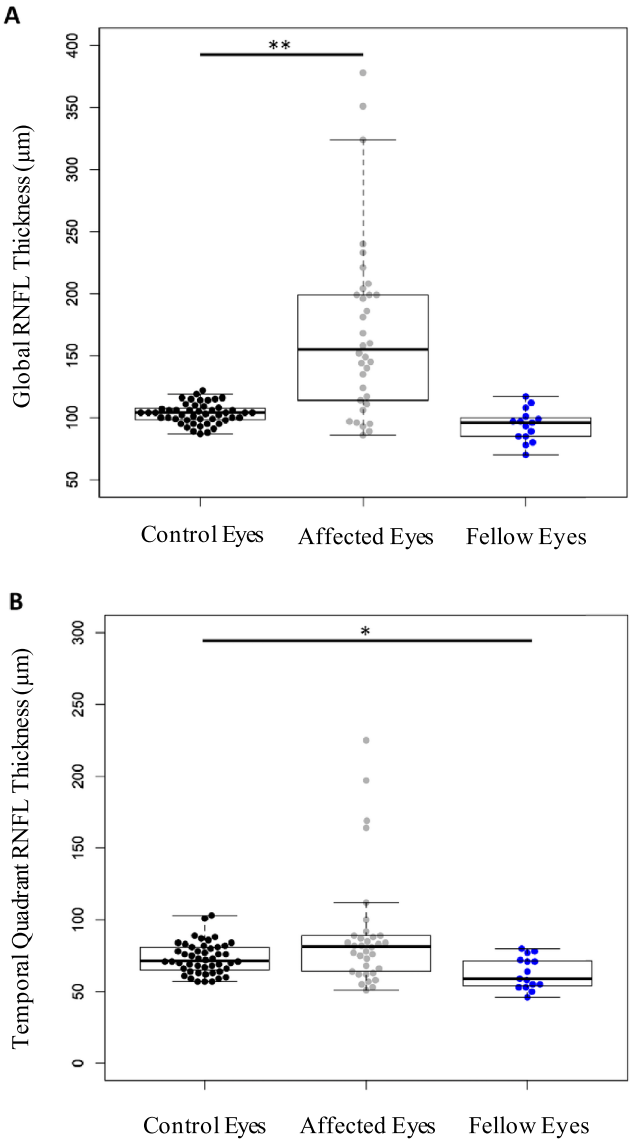

Fig. 3. Distribution of (A) mean retinal nerve fiber layer (RNFL) thickness and (B) temporal quadrant RNFL thickness in control, optic neuritis-affected, and fellow eyes. *$p < 0.01$; **$p < 0.0001$.

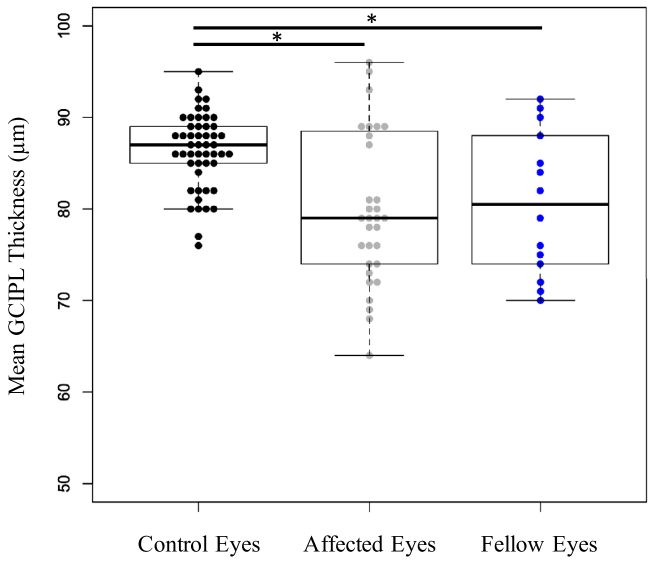

Fig. 4. Distribution of mean ganglion cell/inner plexiform layer (GCIPL) thickness in control, optic neuritis-affected, and fellow eyes. *$p < 0.01$.

3.5. Relationship between OCT measures at presentation and visual function at follow-up

Seventeen ON-participants (23 ON-affected eyes, 11 fellow eyes), including seven with an MS diagnosis, had visual outcome data available (Fig. 2). Among these children, ON-affected eyes had reduced LCVA compared to control eyes (median 1.35 [IQR 1.35–1.5] versus 1.6 [IQR 1.5–1.65], $p < 0.0001$). While a greater proportion of ON-affected eyes at follow-up had abnormal color vision compared to control eyes (9/23 eyes [39%] vs 7/48 eyes [15%], $p = 0.033$), this difference was not significant after correction for multiple comparisons. Neither LCVA in fellow eyes (median 1.5 [IQR 1.35–1.8], $p = 0.85$) nor the proportion of fellow eyes with abnormal color vision (2/11 eyes [22%], $p = 0.67$) differed significantly from control eyes at follow-up.

No significant association was identified between global RNFL thickness (OR = 0.933; 95% CI 0.875, 0.995; $p = 0.034$) or GCIPL thickness (OR = 0.885; 95% CI 0.774, 1.01; $p = 0.07$) at presentation and eyes having abnormal color vision at follow-up. Similarly, there was no association between global RNFL thickness ($\beta = 0.0004$; 95% CI −0.0009, 0.0017; $p = 0.53$) or GCIPL thickness ($\beta = -0.0004$; 95% CI −0.011, 0.011; $p = 0.95$) at presentation and LCVA at follow-up.

Table 2
Optical coherence tomography measures in participant eyes.

	Control Eyes ($N = 50$[a])	ON-Affected Eyes ($N = 35$[a])	p-Value[b]	Fellow Eyes ($N = 15$[a])	p-Value[b]
Global RNFL (µm), median (IQR)	104 (98.5–107.5)	155 (114–199)	< **0.0001**	96 (85–101)	0.029
Superior Quadrant RNFL (µm), median (IQR)	127.5 (120.5–141.5)	212 (158–313)	< **0.0001**	115 (104–120)	0.15
Nasal Quadrant RNFL (µm), median (IQR)	73 (65–80)	123 (80–175)	< **0.0001**	73 (57–84)	0.41
Inferior Quadrant RNFL (µm), median (IQR)	139 (125–148)	207.5 (140–268)	< **0.0001**	122 (111–140)	**0.013**
Temporal Quadrant RNFL (µm), median (IQR)	71.5 (65–81)	81.5 (64–89)	0.10	59 (53–72)	**0.008**
GCIPL (µm), median (IQR)	87 (85–89)	79 (74–88)	**0.003**	80.5 (74–88)	**0.003**

IQR, interquartile range; ON, optic neuritis; RNFL, retinal nerve fiber layer; GCIPL, ganglion cell/inner plexiform layer.

[a] The following number of eyes were included in RNFL analysis: Control = 48, Fellow = 15, ON-Affected = 34. The following number of eyes were included in GCIPL analysis: Control = 50, Fellow = 14, ON-Affected = 31.

[b] P-values for comparison with control eyes obtained from the generalized linear mixed models, adjusting for sex, age, and inter-eye correlations. Bolded values are significant after adjustment for multiple comparisons.

Table 3
Optical coherence tomography measures in the eyes of participants diagnosed with multiple sclerosis compared to those with monophasic demyelination.

	ON-Affected Eyes Multiple Sclerosis ($N = 10$[a])	Monophasic ($N = 25$[a])	p-Value[b]	Fellow Eyes Multiple Sclerosis ($N = 8$[a])	Monophasic ($N = 7$[a])	p-Value[b]
Global RNFL (μm), median (IQR)	108.5 (95–124)	183.5 (146.5–206)	**0.01**	87 (79–95)	101 (96–112)	0.39
Temporal Quadrant RNFL (μm), median (IQR)	74 (62–82)	84 (66–96)	0.15	54 (51.5–64.5)	72 (59–78)	0.40
GCIPL (μm), median (IQR)	79 (75–81)	79 (73–89)	0.96	75 (71.5–86.5)	83 (79–91)	0.40

IQR, interquartile range; ON, optic neuritis; RNFL, retinal nerve fiber layer; GCIPL, ganglion cell/inner plexiform layer.

[a] The following number of eyes were included in RNFL analysis: ON-Affected (MS) = 10, ON-Affected (Monophasic) = 24, Fellow (MS) = 8, Fellow (Monophasic) = 7. The following number of eyes were included in GCIPL analysis: ON-Affected (MS) = 8, ON-Affected (Monophasic) = 23, Fellow (MS) = 8, Fellow (Monophasic) = 6.

[b] P-values for comparison between diagnostic sub-groups obtained from the generalized linear mixed models, adjusting for sex, age, and inter-eye correlations. Bolded values are significant after adjustment for multiple comparisons.

4. Discussion

This prospective cohort study examined OCT measures at presentation in children with ON as part of a first demyelinating event. We found evidence for early neuronal injury in affected eyes, as evidenced by GCIPL thinning, within 30 days of symptom onset in our pediatric ON cohort. We also identified fellow eye abnormalities, including lower inferior RNFL, temporal RNFL, and GCIPL thicknesses than controls, which suggest the presence of pre-existing, subclinical neuroaxonal injury in a subgroup of children presenting with ON. Patterns of OCT changes in the acute phase after ON differed in children diagnosed with MS compared to monophasic demyelination in this study.

GCIPL thickness was significantly lower in both the ON-affected and clinically unaffected (fellow) eyes of children with ON, as compared to healthy controls. Adult studies have previously demonstrated that GCIPL thinning may be seen within one month of ON onset in affected eyes (Kupersmith et al., 2016), while fellow eyes show a stable GCIPL thickness over 6 months following acute ON (Gabilondo et al., 2015). Thus, while the lower GCIPL thickness observed in ON-affected eyes in the current study could reflect early GCIPL thinning as a result of acute ON, the fellow eye abnormalities are not expected to be a result of acute ON. Rather, this lower observed GCIPL thickness – particularly that seen in fellow eyes – could be interpreted to represent a relatively high prevalence of pre-existing afferent visual pathway injury in our pediatric cohort. Furthermore, there were not prominent outliers in fellow eye GCIPL values, suggesting that the lower GCIPL thickness seen in fellow eyes is not simply a reflection of a small number of individuals with extensive pre-existing atrophy. The degree of reduction in GCIPL thickness in this cohort – approximately 8% below the control average – is less than the 10–20% reduction that has been previously reported in cross-sectional studies of children with demyelinating syndromes evaluated 6 months or more after clinical onset (Yeh et al., 2014; Graves et al., 2017), suggesting that further GCIPL declines are expected to occur with time. Whether this indicates a window in which therapeutic intervention has the potential to preserve the integrity of remaining retinal ganglion cells and their axons is unknown.

RNFL thickness was significantly higher in ON-affected eyes compared to healthy controls, which was expected given the high rate of papillitis observed in pediatric ON cohorts (Wilejto et al., 2006; Bonhomme et al., 2009). Conversely, RNFL thickness – most significantly in the inferior and temporal quadrants – was lower in fellow eyes compared to controls. This lower RNFL thickness correlated strongly with lower GCIPL thickness in fellow eyes and, together with the GCIPL findings, supports the presence of pre-existing neuroaxonal injury in the afferent visual pathway within a subset of children in this cohort. RNFL swelling related to stasis of axoplasmic flow resulting from acute optic nerve inflammation may have masked the presence of early axonal loss in ON-affected eyes (Kupersmith et al., 2011). Thus, GCIPL thinning may be the more appropriate early marker of neuroaxonal injury after pediatric ON, as has been suggested from adult studies (Kupersmith et al., 2016).

Children with MS had a lower global RNFL thickness in their ON-affected eyes than did children with monophasic demyelination. This may, in part, reflect a lower capacity for swelling within the optic nerves of children with MS due to the presence of pre-existing neuroaxonal injury and consequently fewer viable axons at the time of ON. The presence of pre-existing, subclinical neuroaxonal injury in those children with MS is supported by previous studies that have demonstrated reductions in RNFL and GCIPL thickness in eyes both with and without a history of ON outside of the acute period (Petzold et al., 2017; Yeh et al., 2014, 2009; Gelfand et al., 2012; Waldman et al., 2017). Indeed, in this study we found the fellow eyes of children with MS to have lower global RNFL, temporal RNFL, and GCIPL measures than their monophasic counterparts. These fellow eye differences were not statistically significant; however, the small number of fellow eyes in this study limited the power to show differences between the diagnostic sub-groups. The presence of GCIPL and RNFL thinning in fellow eyes at the time of a first clinical event, particularly in those children with MS, suggests that, like their adult counterparts, children with MS are vulnerable to subclinical neuroaxonal damage early in their disease course (Petzold et al., 2017). Importantly, this suggests that a simple, non-invasive technology – OCT – may discern distinctive structural patterns in children with MS within 30 days of their first clinical event.

Conversely, GCIPL thickness in ON-affected eyes was similar between MS and monophasic participants. This finding does not support the conclusion of pre-existing neuroaxonal injury primarily in those children with MS. Given the more pronounced RNFL swelling in the ON-affected eyes of the monophasic group, this could reflect an artifactual lowering of measured GCIPL thickness due to anatomical distortion in the context of significant optic disk edema within the monophasic group (OCT Sub-Study Committee for the NORDIC Idiopathic Intracranial Hypertension Study Group 2014). However, we did not find a correlation between higher global RNFL thickness and lower GCIPL thickness in ON-affected eyes, suggesting that the lower GCIPL thickness is a true – not artifactual - decrease. Previous studies in the chronic phase following ON have found lower GCIPL thickness in the ON-affected eyes of children and adults with anti-MOG seropositive ON compared to those with seronegative ON or MS (Chen et al., 2018; Sotirchos et al., 2019). Thus, it is possible that more prominent early GCIPL loss as a consequence of acute ON in those children with monophasic demyelination (a portion of whom were anti-MOG seropositive) obscured the difference expected from the presence of pre-existing GCIPL injury in those children with MS. Given the small sample size in the current study, further studies are required to address the potential differences in acute OCT measures between children with MS and those with anti-MOG antibody-associated demyelination.

As a secondary objective, we investigated the relationship between initial OCT measures and follow-up visual outcomes in children with

ON. LCVA remained worse in ON-affected eyes at follow-up compared to controls. Neither RNFL nor GCIPL thickness at onset was significantly associated with functional visual outcomes at follow up, although the small numbers of eyes with adverse visual outcomes limited the ability to detect such associations. Prospective longitudinal studies are necessary to assess whether decrements in RNFL and/or GCIPL thickness over time, rather than a single acute measure, better predict visual outcomes after pediatric ON, as has been demonstrated in adult studies (Sanchez-Dalmau et al., 2018).

This study has several limitations, including a relatively small sample size that limits the power to perform sub-group analyses, particularly in regard to fellow eyes given the high rate of bilateral ON. Conclusions regarding the differing pattern of injury in children with MS should be interpreted with caution, given the small number of MS subjects and heterogeneity within the monophasic demyelinating group that included both anti-MOG antibody seropositive and seronegative children, as well as those who may potentially develop recurrent disease given a longer period of clinical follow-up. Attempts should thus be made to replicate these findings in larger cohorts. Finally, previous studies in NMOSD and MOG-associated ON have suggested that early intervention with intravenous methylprednisolone may be associated with improved visual recovery and preserved RNFL thickness (Stiebel-Kalish et al., 2019; Nakamura et al., 2010). Whether the variability in the timing of treatment with intravenous methylprednisolone in relation to ON onset and OCT testing in the current study may have influenced acute OCT measures or the ability to associate these measures with long-term visual outcomes is unknown.

4.1. Conclusion

Evidence for early neuroaxonal injury in children with ON can be detected at first presentation in both their clinically affected and fellow eyes. Larger studies are needed to confirm whether the presence of such early injury on OCT may be used as a surrogate marker to predict clinical outcomes in children.

Declaration of Competing Interest

DLA reports consultant fees and/or grants outside of the submitted work from Acorda, Adelphi, Alkermes, Biogen, Celgene, Frequency Therapeutics, Genentech, Genzyme, Hoffman LaRoche, Immune Tolerance Network, Immunotec, MedDay Merck-Serono, Novartis, Pfizer, Receptos, Roche, Sanofi-Aventis, Canadian Institutes of Health Research, MS Society of Canada, International Progressive MS Alliance, and an equity interest in NeuroRx Research. RAM reports grants from the MS Scientific Research Foundation, Canadian Institutes of Health Research, MS Society of Canada, National MS Society, Consortium of MS Centers, Research Manitoba, and Crohn's and Colitis Canada during the conduct of this study. FC reports personal fees from Clene and EMD Serono, outside the submitted work. EAY reports the following, outside of the submitted work: funding from the National MS Society, Canadian Institute for Health Information, Canadian Institutes of Health Research, Ontario Intitute for Regenerative Medicine, MS Society of Canada, Mario Battaglia Foundation, SickKids Foundation, Centre for Brain and Mental Health Innovation Fund, Consortium of Multiple Sclerosis Centers, Rare Diseases Foundation, and Guthy Jackson Foundation. She serves as a relapse adjudicator for ACI and has served on scientific advisory panels for Juno Therapeutics, Alexion, and Hoffman-Laroche.

Acknowledgments

The authors wish to acknowledge Shiyi Chen, Derek Stephens, and Mamadou Diallo for assistance with statistical analysis and to thank Austin Noguera, Julia O'Mahony, Danusha Nandamalavan, and Renisha Iruthayanathan for their contributions to patient recruitment, data collection, and database maintenance. Collaborators part of the Canadian Pediatric Demyelinating Disease Network are recognized in Supplemental Table 1.

Funding sources

This study was supported by funding from the Ontario Institute for Regenerative Medicine, Stem Cell Network (grant no. DT12), Multiple Sclerosis Scientific Research Foundation (grant no. 2352), Canadian Institutes of Health Research – Canada Graduate Scholarships, SickKids Research Institute, and the SickKids Foundation. The study funders were not involved in study design, analysis/interpretation of data, writing of the manuscript, nor the decision to submit for publication.

Supplementary materials

Supplementary material associated with this article can be found, in the online version, at doi:10.1016/j.msard.2019.101387.

References

Absoud, M., Cummins, C., Desai, N., et al., 2011. Childhood optic neuritis clinical features and outcome. Arch. Dis. Child 96 (9), 860–862.
Banwell, B., Kennedy, J., Sadovnick, D., et al., 2009. Incidence of acquired demyelination of the CNS in Canadian children. Neurology 72 (3), 232–239.
Benjamini, Y., Hochberg, Y., 1995. Controlling the false discovery rate: a practical and powerful approach to multiple testing. J. R. Stat. Soc. Ser. B Stat. Methodol. 57 (1), 289–300.
Bonhomme, G.R., Waldman, A.T., Balcer, L.J., et al., 2009. Pediatric optic neuritis: brain MRI abnormalities and risk of multiple sclerosis. Neurology 72 (10), 881–885.
Chandrakumar, M., Colpa, L., Reginald, Y.A., et al., 2013. Measuring contrast sensitivity using the M&S Smart System II versus the Pelli–Robson chart. Ophthalmology 120 (10), 2160–2161 e1.
Chen, Q., Zhao, G., Huang, Y., et al., 2018. Clinical characteristics of pediatric optic neuritis with myelin oligodendrocyte glycoprotein seropositive: a cohort study. Pediatr. Neurol. 83, 42–49.
Costello, F., Burton, J.M., 2018. Retinal imaging with optical coherence tomography: a biomarker in multiple sclerosis? Eye Brain 10, 47–63.
Costello, F., Coupland, S., Hodge, W., et al., 2006. Quantifying axonal loss after optic neuritis with optical coherence tomography. Ann. Neurol. 59 (6), 963–969.
Costello, F., Pan, Y.I., Yeh, E.A., et al., 2015. The temporal evolution of structural and functional measures after acute optic neuritis. J. Neurol. Neurosurg. Psychiatry 86 (12), 1369–1373.
Ferris, F.L., Kassoff, A., Bresnick, G.H., Bailey, I., 1982. New visual acuity charts for clinical research. Am. J. Ophthalmol. 94 (1), 91–96.
Gabilondo, I., Martinez-Lapiscina, E.H., Fraga-Pumar, E., et al., 2015. Dynamics of retinal injury after acute optic neuritis. Ann. Neurol. 77 (3), 517–528.
Gelfand, J.M., Goodin, D.S., Boscardin, W.J., et al., 2012. Retinal axonal loss begins early in the course of multiple sclerosis and is similar between progressive phenotypes. PLoS ONE 7 (5), e36847.
Graves, J.S., Chohan, H., Cedars, B., et al., 2017. Sex differences and subclinical retinal injury in pediatric-onset MS. Mult. Scler. 23 (3), 447–455.
Holmes, J.M., Beck, R.W., Repka, M.X., et al., 2001. The amblyopia treatment study visual acuity testing protocol. Arch. Ophthalmol. 119 (9), 1345–1353.
Knier, B., Berthele, A., Buck, D., et al., 2016. Optical coherence tomography indicates disease activity prior to clinical onset of central nervous system demyelination. Mult. Scler. 22 (7), 893–900.
Krupp, L.B., Tardieu, M., Amato, M.P., et al., 2013. International pediatric multiple sclerosis study group criteria for pediatric multiple sclerosis and immune-mediated central nervous system demyelinating disorders: revisions to the 2007 definitions. Mult. Scler. 19 (10), 1261–1267.
Kupersmith, M.J., Garvin, M.K., Wang, J.-K., et al., 2016. Retinal ganglion cell layer thinning within one month of presentation for optic neuritis. Mult. Scler. 22 (5), 641–648.
Kupersmith, M.J., Mandel, G., Anderson, S., et al., 2011. Baseline, one and three month changes in the peripapillary retinal nerve fiber layer in acute optic neuritis: relation to baseline vision and MRI. J. Neurol. Sci. 308 (1–2), 117–123.
Lechner, C., Baumann, M., Hennes, E.M., et al., 2016. Antibodies to MOG and AQP4 in children with neuromyelitis optica and limited forms of the disease. J. Neurol. Neurosurg. Psychiatry 87 (8), 897–905.
Meltzer, E.I., Costello, F.E., Frohman, E.M., Frohman, T.C., 2018. New ways of “seeing” the mechanistic heterogeneity of multiple sclerosis plaque pathogenesis. J. Neuroophthalmol. 38 (1), 91–100.
Mwanza, J.C., Oakley, J.D., Budenz, D.L., Chang, R.T., Knight, O.J., Feuer, W.J., 2011. Macular ganglion cell-inner plexiform layer: automated detection and thickness reproducibility with spectral domain-optical coherence tomography in glaucoma. Invest Ophthalmol. Vis. Sci. 52 (11), 8323–8329.
Nakamura, M., Nakazawa, T., Doi, H., et al., 2010. Early high-dose intravenous methylprednisolone is effective in preserving retinal nerve fiber layer thickness in patients

with neuromyelitis optica. Graefes Arch. Clin. Exp. Ophthalmol. 248 (12), 1777–1785 2010.
OCT Sub-Study Committee for the NORDIC Idiopathic Intracranial Hypertension Study Group, 2014. Baseline OCT measurements in the idiopathic intracranial hypertension treatment trial, part I: quality control, comparisons, and variability. Invest. Ophthalmol. Vis. Sci. 55 (12), 8180–8188.
Petzold, A., Balcer, L.J., Calabresi, P.A., et al., 2017. Retinal layer segmentation in multiple sclerosis: a systematic review and meta-analysis. Lancet Neurol. 16 (10), 797–812.
Pohl, D., Rostásy, K., Treiber-Held, S., et al., 2006. Pediatric multiple sclerosis: detection of clinically silent lesions by multimodal evoked potentials. J. Pediatr. 149 (1), 125–127.
Sanchez-Dalmau, B., Martinez-Lapiscina, E.H., Torres-Torres, R., et al., 2018. Early retinal atrophy predicts long-term visual impairment after acute optic neuritis. Mult. Scler. 24 (9), 1196–1204.
Schippling, S., Balk, L.J., Costello, F., et al., 2015. Quality control for retinal OCT in multiple sclerosis: validation of the OSCAR-IB criteria. Mult. Scler. 21 (2), 163–170.
Sotirchos, E.S., Filippatou, A., Fitzgerald, K.C., et al., 2019. Aquaporin-4 IGG seropositivity is associated with worse visual outcomes after optic neuritis than MOG-IGG seropositivity and multiple sclerosis, independent of macular ganglion cell layer thinning. Mult. Scler. https://doi.org/10.1177/1352458519864928. [ePub ahead of print].
Stiebel-Kalish, H., Hellmann, M.A., Mimouni, M., et al., 2019. Does time equal vision in the acute treatment of a cohort of AQP4 and MOG optic neuritis? Neurol. Neuroimmunol. Neuroinflamm. 6 (4), e572.
Tewarie, P., Balk, L., Costello, F., et al., 2012. The oscar-ib consensus criteria for retinal OCT quality assessment. PLoS ONE 7 (4), e34823.
Waldman, A.T., Liu, G.T., Lavery, A.M., et al., 2017. Optical coherence tomography and visual evoked potentials in pediatric MS. Neurol. Neuroimmunol. Neuroinflamm. 4 (4), e356.
Waters, P., Woodhall, M., O'Connor, K.C., et al., 2015. MOG cell-based assay detects non-MS patients with inflammatory neurologic disease. Neurol. Neuroimmunol. Neuroinflamm. 2 (3), e89.
Waters, P.J., Pittock, S.J., Bennett, J.L., et al., 2014. Evaluation of aquaporin-4 antibody assays. Clin. Exp. Neuroimmunol. 5 (3), 290–303.
Wilejto, M., Shroff, M., Buncic, J.R., et al., 2006. The clinical features, MRI findings, and outcome of optic neuritis in children. Neurology 67 (2), 258–262.
Wingerchuk, D.M., Banwell, B., Bennett, J.L., et al., 2015. International consensus diagnostic criteria for neuromyelitis optica spectrum disorders. Neurology 85 (2), 177–189.
Yeh, E.A., Marrie, R.A., Reginald, Y.A., et al., 2014. Functional-structural correlations in the afferent visual pathway in pediatric demyelination. Neurology 83 (23), 2147–2152.
Yeh, E.A., Weinstock-Guttman, B., Lincoff, N., et al., 2009. Retinal nerve fiber thickness in inflammatory demyelinating diseases of childhood onset. Mult. Scler. 15 (7), 802–810.